J Therm Anal Calorim (2010) 101:737–742
DOI 10.1007/s10973-010-0869-7

Structural, thermal, and electrical properties of carbonaceous films containing palladium nanocrystals

E. Kowalska · E. Czerwosz · M. Kozłowski · W. Surga · J. Radomska · H. Wronka

IVMTT2009 Special Chapter
© Akadémiai Kiadó, Budapest, Hungary 2010

Abstract Carbonaceous films containing Pd nanocrystals can be applied as active layers in gas sensor applications. In this article we show results of studies of C-Pd films, obtained with two different methods: (1) physical and (2) physical + chemical deposition. First type of film prepared by physical vapor deposition (PVD) process was composed of fullerenes, amorphous carbon, and palladium nanograins. In the second method PVD film was modified in chemical vapor deposition (CVD) process forming a foam-like structure. Both types of films were studied by SEM, TEM, TGA, and electrical characterization (measurement of resistivity versus composition of gaseous hydrocarbons mixture).

Keywords Carbonaceous-palladium film · Carbon foam · Thermal stability · Hydrogen sensor

Introduction

Gas sensors are devices to detect or to measure concentration of different gaseous components in ambient atmosphere. In industrial production of chemical compounds, automotive transport, glass treatment, cryogenic cooling, as well as in petroleum conversion, hydrogen sensors are of great importance because they decide on a work safety and a human life. Requirements of a H_2 sensor are as follows: high sensitivity, fast response, high selectivity, long lifetime, operational safety, and low power consumption. A low electrical power can be achieved by sensor miniaturization. Therefore, researches pay their attention on nanomaterials, which are considered as ideal building blocks for gas adsorption and chemical gas sensing.

Nanostructured materials have developed specific surface area that allows to improve gas sensor sensitivity. Apart from, their small size, density, and weight cause lower consumption of raw materials, thus lower commercial production cost. Recently, carbon nanotubes (CNTs) have been utilized as an active sensing element in detection of hydrogen [1], NH_3, NO_2 [2, 3], and also of volatile organic compounds (such as ethanol, ethyl acetate, and toluene in nitrogen) [4]. CNT active element was built from pristine CNTs [5], CNTs filled with metal clusters [6, 7], and CNTs coated with polymers [2].

The other promising nanomaterials that can be used as gas sensing layers are carbon foams. The carbon foam includes a network of pores into which gaseous atoms or molecules could be adsorbed [8]. The carbon foam resists corrosion and exhibits high mechanical strength and thermal resistance, low density ($0.2 \div 0.8$ gcm^3) due to the presence of micro-, meso-, or macropores. These pores form highly developed surface area (of the order of hundred m^{2}g) [9]. These properties enable to utilize carbon nanoporous materials in gas sensors as active elements or as electrodes in batteries or fuel cells as well as in catalysis, ion exchange, molecular segregation, and insulation. Therefore, new effective production methods of carbon foams are still searched for. Initially, carbon foams were formed by the pyrolysis of thermosetting polymer [10, 11]. At present there are many various precursors for production of lightweight carbon materials such as coal, coal tar pitch,

E. Kowalska (✉) · E. Czerwosz · M. Kozłowski · J. Radomska · H. Wronka
Tele and Radio- Research Institute, 11 Ratuszowa Street, 03-450 Warsaw, Poland
e-mail: ewa.kowalska@itr.org.pl

W. Surga
Institute of Chemistry, Jan Kochanowski University, 15 G Świętokrzyska Street, 25-406 Kielce, Poland

petroleum pitch [9], polyimide [12], mixture of alcohols (hexadecanol/octadecanol/furfuryl alcohol–surfactant mixture) [13]. Recently, the high repetition rate laser ablation of a glassy carbon target in non-reactive argon atmosphere has been applied to the formation of carbon nanoporous structures [14]. The thermal and thermomechanical properties of different types of foams were presented in [15–17].

In this article we describe results of topography, morphology (SEM: Scanning Electron Microscopy), structure (TEM: Transmission Electron Microscopy), and thermal stability (TGA: Thermogravimetric Analysis) of polycrystalline multiphase C-Pd films obtained by PVD (Physical Vapor Deposition) method and a foam-like C-Pd films, prepared by two stages process based on PVD and CVD (Chemical Vapor Deposition) [18]. This kind of carbon nanomaterials containing Pd nanograins can be applied as active layers in hydrogen gas sensors not only due to a high specific carbon surface area but also because of the presence of Pd nanoparticles that adsorb selectively hydrogen gas and form palladium hydride (PdH_x). The resistance of PdH_x is different from resistance of the pure Pd metal, and this effect could be used as a factor to detect hydrogen or hydrogen compounds. Electrical properties of prepared films were investigated in a vacuum chamber adapted to measure the sample's resistance in the atmosphere of gaseous hydrocarbons mixture.

Experimental

Sample preparation

In PVD method multiphase carbonaceous nano-Pd films were deposited on ceramic substrates under the dynamic pressure of 10^{-5} mbar. Two separated sources were used: one containing fullerene C_{60} powder (99.6%) and second with palladium acetate $Pd(C_2H_3O_2)_2$. During the synthesis process the temperature of the substrates was $\sim$100 °C and growing time was 8 min. The distance between the substrates and sources was 54 mm.

The film originating from PVD process (named PVD film/sample) was modified in CVD method due to temperature and xylene decomposition over the film surface. CVD modification was performed in a horizontal quartz tube reactor placed in a furnace under argon atmosphere and at the reaction temperature of 650 °C. Xylene was introduced into the reaction zone by argon flow. The total reaction time was 30 min. The argon flow rate was maintained at 40 L h^{-1} while xylene flow rate was 0.1 mL min^{-1}. After stopping the flow of xylene the substrates still remained in the furnace in the reaction temperature during 15 min in order to remove a residue of a solvent. Next furnace was cooled to ambient temperature. Finally a carbon nanoporous film-like foam structure containing Pd nanograins was obtained (named CVD film/sample). Experimental CVD setup is presented in Fig. 1.

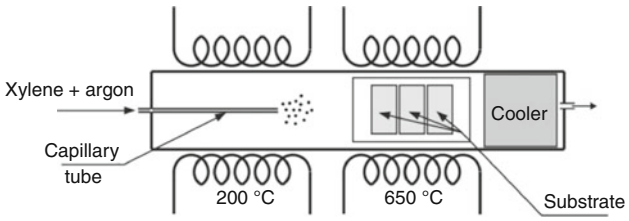

Fig. 1 Scheme of experimental CVD setup

Measurements

The morphology of both types of films (PVD and CVD) was studied by SEM-1530 Leo Gemini with the operating voltage 3 kV and magnification from 1,000 to 250,000×. The structures of PVD and CVD films were investigated by TEM-Jeol JEM 2000 EX operating with 200 keV electron beam energy and with magnification from 10,000 to 400,000×. TEM observation was performed in a bright and a dark field technique. TG measurements of both prepared films were performed using TGA/SDTA 851e Mettler Toledo at the heating rate of 10 °C min^{-1} in nitrogen atmosphere at the flow rate of 2 dm^3 h^{-1}. Derivative thermogravimetric curves were obtained by differential calculations of TG curves.

For PVD and CVD films changes of resistivity in the atmosphere of hydrocarbons mixture were measured in the vacuum chamber shown in Fig. 2. The resistance was measured as a voltage drop on 0.51 MΩ standard resistor. The chemical constitution of a gaseous mixture was composed of nitrogen (70%) and methane (5%), ethane (5%), propane (5%), butane (5%), acetylene (5%), and ethylene

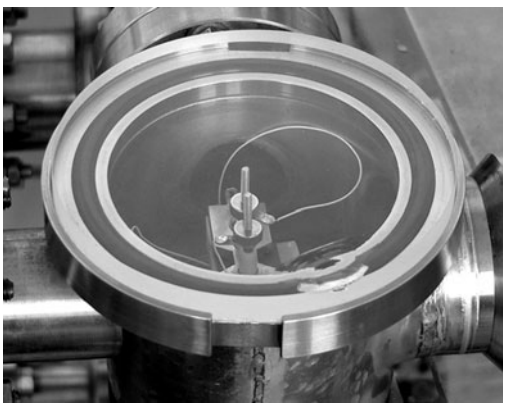

Fig. 2 The vacuum chamber. The substrate with a prepared film is connected with the outer DC supplier

(5%) (sum of hydrocarbons equaled 30% of total gases volume). In order to obtain various concentrations of hydrocarbons, the gaseous mixture was diluted by pure nitrogen. The investigation was performed in an atmospheric pressure under a static condition (the chamber was filled by a mixture of hydrocarbons and nitrogen).

Results and discussion

SEM and TEM investigations

Scanning electron microscope images of PVD film are shown in Fig. 3. In this figure it is seen that the film is built of nanograins. Convex islands possess different sizes, but a large majority of them has a diameter of 60 ÷ 70 nm. Nanograins have sharp edges and smooth walls. Our previous studies by X-ray diffraction method [19] showed that PVD film had a complicated structure and was composed of an amorphous carbon, C_{60}, Pd nanoparticles and organic compounds connected with $Pd(C_2H_3O_2)_2$. Size limit related to X-ray diffraction did not allow us to observe reflexes attributed to interplanar distances of Pd nanocrystals, but TEM image and electron diffraction pattern for selected area (SAED) presented in Fig. 4 confirm the presence of palladium nanoclusters in the PVD film. Registered SAED reflexes (Fig. 4b) are correlated to fcc fullerite C_{60} and fcc Pd nanocrystallites. Pd nanoparticles (dark dots) strongly dispersed in carbonaceous matrix are clearly seen in Fig. 4a.

The size distribution of Pd nanocrystals for the PVD film is shown in Fig. 5. This histogram indicates that a diameter of metal nanocystallites is in the range of 3 ÷ 10 nm, but diagram fitting with Gaussian curve gives a mean size of 4.3 nm.

The film structure modified in CVD process is shown as SEM images in Fig. 6. We can see that after modification roughness of the crystalline PVD film becomes lower and a boundary of crystallites becomes less visible. In Fig. 6b (SEM image with higher magnification) a structure foam-like with pores about different sizes can be observed. TEM measurements of the foam (Figs. 7, 8) show that SAED reflexes related to the fullerite structure (seen in PVD film) disappear and the reflexes attributed to the graphite-like structure appear in the CVD sample. After CVD modification Pd nanograins are enclosed in graphite shells. The graphite grains could be created as a result of decomposition of fullerene/organic compounds or xylene applied in the CVD process.

The size distribution of Pd nanocrystallites for CVD film is presented in Fig. 9, a mean size of nanocrystal is 6.23 nm. These results indicate that CVD process impacts on the palladium size clusters and causes the increase of theirs diameters (of about 16%). This effect is generated by diffusion and aggregation of metal nanocrystals in carbon

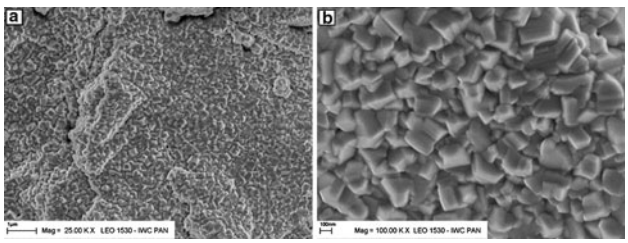

Fig. 3 SEM images of PVD sample deposited on a ceramic substrate: **a** 25,000× and **b** 100,000×

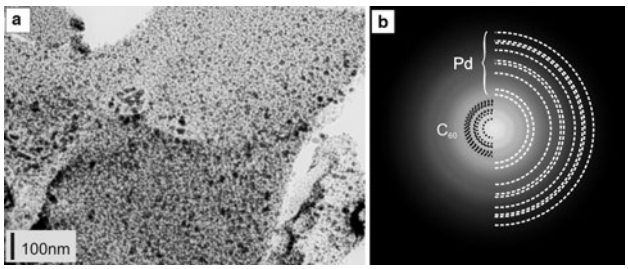

Fig. 4 TEM image of PVD sample: **a** in a bright field technique and **b** electron diffraction patterns attributed to fcc fullerite C_{60} and fcc Pd nanocrystals

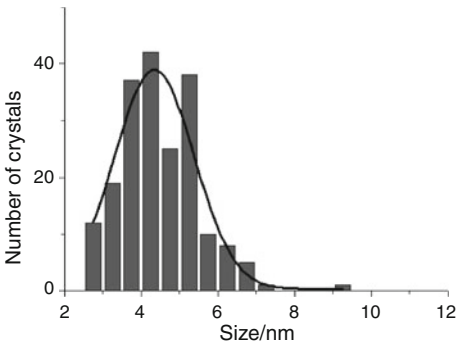

Fig. 5 The size distribution of Pd nanocrystals for PVD sample

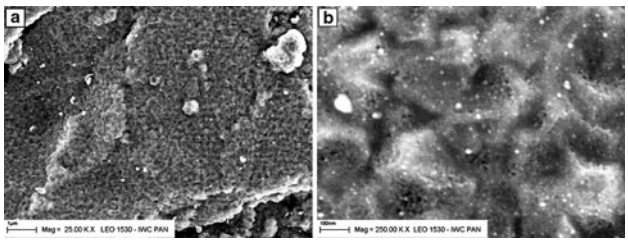

Fig. 6 SEM images of CVD sample obtained in two stages method based on both PVD and CVD processes: **a** 25,000× and **b** 250,000×

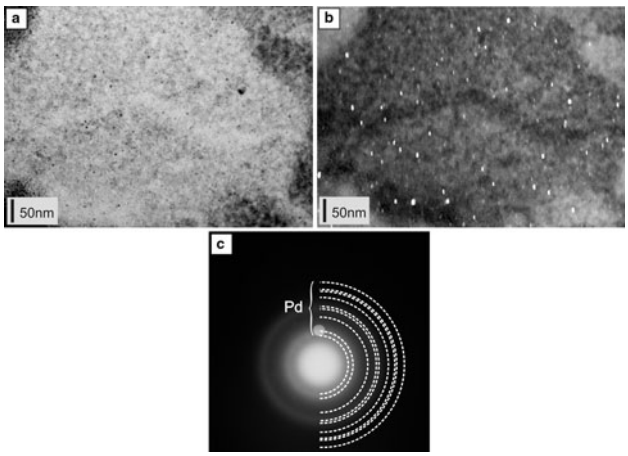

Fig. 7 TEM images of CVD sample: **a** in a bright field technique, **b** in a dark field technique, and **c** electron diffraction patterns attributed to Pd nanocrystallites

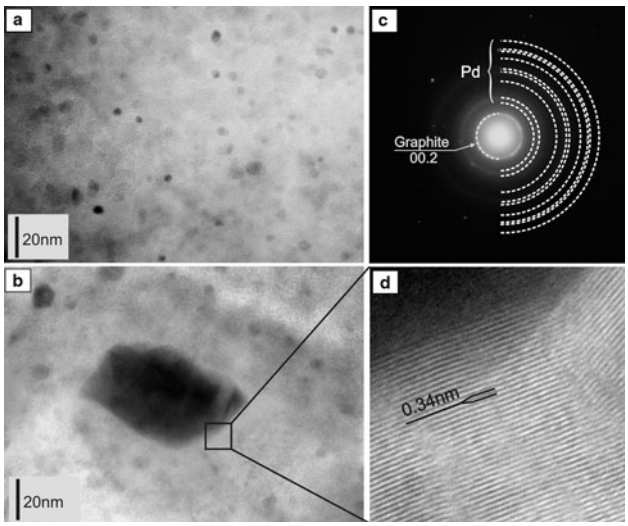

Fig. 8 TEM images of CVD sample: **a**, **b** in a bright field technique, **c** electron diffraction patterns related to the graphite structure, and **d** a structure fragment from **b** with higher magnification

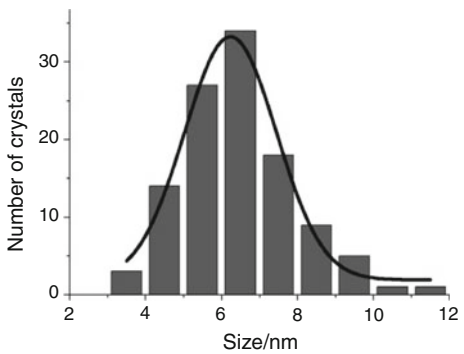

Fig. 9 The size distribution of Pd nanocrystals for CVD sample

matrix under the influence of temperature in the CVD method. CVD process also converts the polycrystalline PVD films into porous carbon nanomaterials.

TG measurements

TG and DTG curves for both PVD and CVD films are shown in Figs. 10 and 11, respectively. These curves demonstrate that the total mass loss of PVD sample (60.8 wt%) proceeds in two-step process with maximum on the DTG curve at the temperature of about 200 °C (11.7 wt% mass loss) and 650 °C (39.8 wt% mass loss). Between this temperature ranges the uniform mass loss is recorded. The first degradation step is probably connected with the evaporation of a residue of Pd acetate (temperature decomposition of $Pd(CH_3COO)_2$ is about 205 °C [20]). Uniform mass loss could be related to a residue of different organic compounds and radicals created during PVD process from decomposition of C_{60} and $Pd(CH_3COO)_2$. And final mass loss (650 °C) could be attributed to fullerene (it is known that temperature of C_{60} sublimation is about

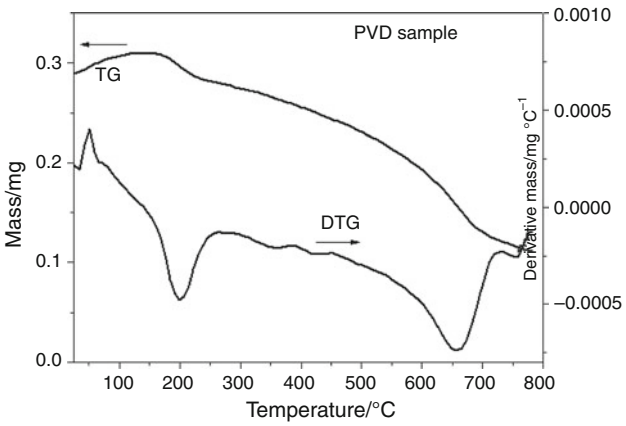

Fig. 10 TG and DTG curves of PVD sample

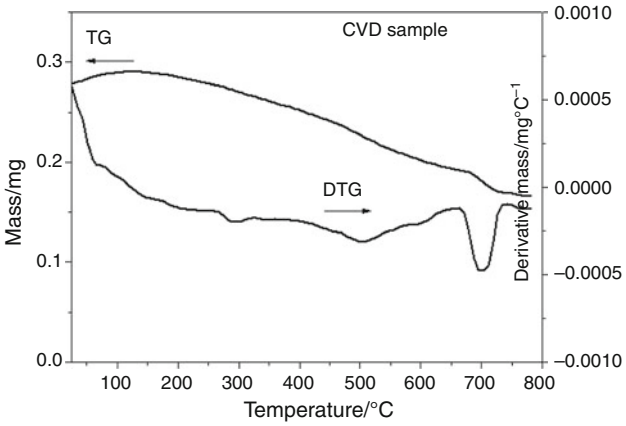

Fig. 11 TG and DTG curves of CVD sample

600 °C [21]). We suppose that the final effect might be also correlated with the mass loss connected with changes in interface between palladium nanocrystallites and carbon matrix under the influence of temperature. Because the similar behavior at this temperature was observed too in the CVD sample (recorded mass loss at 650 °C is 10.9 wt%, Fig. 11, it is smaller than for the multiphase film) for which TEM observations confirm the decay of reflexes attributed to fcc fullerite C_{60}.

The total mass loss (39.3 wt%) of the foam-like structure is much less than for the initial PVD sample. We suggest that the uniform mass loss observed from ambient temperature to 800 °C for the modified sample can be related to evaporation of a residue of xylene or other hydrocarbons which could be formed as result of polymerization of hydrocarbon radicals in the CVD process. These radicals could be created due to xylene thermal decomposition. The results indicate that time of heating ~15 min (after CVD modification) is too short to remove the residue of all hydrocarbons. We suggest that time of heating CVD samples should be longer than 15 min or the temperature should be higher than 650 °C.

Electrical properties

The electrical properties of PVD and CVD films were measured in following order:

1. the substrate with the film was installed in the vacuum chamber and was connected with the outer DC supplier
2. the vacuum chamber was purified from residual gases until to the vacuum of 10^{-5} mbar
3. the mixture of hydrocarbons (30% of hydrocarbons and 70% of nitrogen) was introduced into the vacuum chamber for achievement of a proper pressure level. The pressure of gaseous mixture was registered
4. pure nitrogen was introduced into the chamber up to an atmospheric pressure
5. the sample resistance in the medium of a gaseous mixture was measured as a function of duration time
6. after measurements in hydrocarbons atmosphere the chamber was filled by air and a sample resistance was again recorded.

From the result of these studies, we find that both films are sensitive to a gas containing hydrogen compounds but with different dependencies. The difference of resistivity ΔR (between resistivity measured in the gas and in a vacuum) for PVD and CVD samples are presented in Figs. 12 and 13, respectively.

Results indicate that PVD film resistivity (ΔR) shows nearly linear decrease with increasing concentration of hydrocarbons (Fig. 12), but the high resistance of this film disables its application for hydrogen detection. Resistance

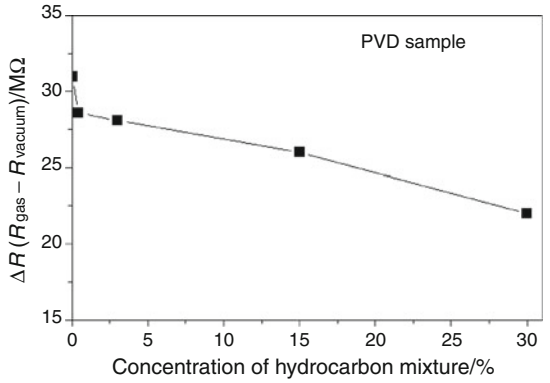

Fig. 12 The difference of resistivity ΔR ($R_{gas} - R_{vacuum}$) for PVD film measured versus of the gaseous mixture concentration

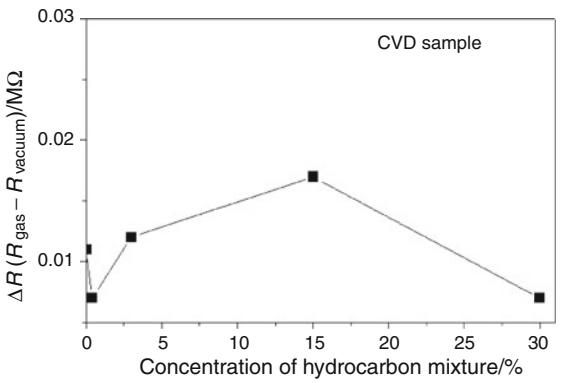

Fig. 13 The difference of resistivity ΔR ($R_{gas} - R_{vacuum}$) for CVD film measured versus of the gaseous mixture concentration

of the sample after CVD modification (Fig. 13) is about thousand times lower than for the initial PVD film.

The decrease of resistivity (ΔR) for the foam sample in the atmosphere of hydrocarbons could be connected with high surface area development. This high development is caused by CVD parameters acting on a growth process that forms the surface. On the other hand this decrease of resistivity could be related to swelled nanosized palladium crystals when hydrogen compounds are adsorbed [22]. Some Pd nanocrystals probably form new electrical connections with their neighborhood during the process of expansion [23]. The increased number of conducting pathways could cause a decrease in the film resistance. Our results show that the CVD film can be used as an active layer in hydrogen or hydrocarbon sensor device.

Conclusions

Here we present here preliminary results of studies on the carbon–metal nanomaterials properties. Initial polycrystalline carbonaceous nano-Pd films modified in CVD process are converted into carbon nanoporous films with foam-

like structure. This new class of carbon nanomaterials could be used as an active element in hydrogen and hydrocarbons detection. It shows the high sensitivity to the presence of hydrocarbon gases in the surroundings.

Our prediction is connected with observed highly developed surface of the films and with the presence of Pd nanocrystallites on their surface. These two factors are very important for sensitivity of chemically hydro-active films.

Acknowledgements This research was co-financed by the European Regional Development Fund within the Innovative Economy Operational Programme 2007-2013 ("Development of technology for a new generation of the hydrogen and hydrogen compounds sensor for applications in above normative conditions", No UDA-POIG.01.03.01-14-071/08-00) No UDA-POIG.01.03.01-14-071/08-00).

References

1. Sinha N, Ma J, Yeow JTW. Carbon nanotube based sensor. J Nanosci Nanotechnol. 2006;6(3):573–90.
2. Kong J, Franklin NR, Zhou C, Chapline MG, Peng S, et al. Nanotube molecular wires as chemical sensors. Science. 2000;287:622–5.
3. Zhao J, Buldum A, Han J, Lu JP. Gas molecule adsorption in carbon nanotubes and nanotube bundles. Nanotechnology. 2002;13: 195–200.
4. Penza M, Antolini F, Vittori MA. Carbon nanotubes as SAW chemical sensors materials. J Sens Actuators B. 2004;100:47–59.
5. Li J, Lu Y, Ye Q, Cinke M, Han J, Meyyappan M. Carbon nanotube sensors for gas and organic vapor detection. Nano Letters. 2003;3(7):929–33.
6. Lu Y, Li J, Han J, Ng H-T, Binder C, Partridge C, Meyyappan M. Room temperature methane detection using palladium loaded singlewalledcarbon nanotube sensors. Chem Phys Lett. 2004;391:344–8.
7. Young P, Lu Y, Terrill R, Li J. High sensitivity NO_2 detection with carbon nanotubes - gold nanoparticle composite films. J Nanosci Nanotechnol. 2005;5(9):1509–12.
8. Rode AV, Hyde ST, Gamaly EG, et al. Structural analysis of a carbon foam formed by a high pulse-rate laser ablation. Appl Phys A. 1999;69:S755–9.
9. Chen Ch, Kennel EB, Stiller AH, et al. Carbon foam derived from various precursors. Carbon. 2006;44:1535–43.
10. Ford WD: US Patent 3121050. 1964.
11. Googin J, Napier J, Scrivner M: US Patent 3345440. 1967.
12. Inagaki M, Morishita T, Kuno A, et al. Carbon foams prepared from polyimide using urethane foam template. Carbon. 2004;42:497–502.
13. Ying JY, Garcia-Martinez J, Lancaster TM: US Patent Pub. No. WO/2005/102964. 2005.
14. Rode AV, Elliman RG, Gamaly EG, et al. Electronic and magnetic properties of carbon nanofoam produced by high-repetitionrate laser ablation. Appl Surf Sci. 2002;197–198:644–9.
15. Gjurova K, Troev K, Bechev Chr, Borisov G. Thermal behavior of rigid polyurethane foams. J Therm Anal. 1986;31:853–9.
16. Gjurova K, Troev K, Bechev Chr, Borisov G. A study of rigid polyurethane foam containing reactive antypirenes. J Therm Anal. 1987;32:97–105.
17. Hakateyama H, Kosugi R, Hatakeyama T. Thermal properties of lignin-and molasses-based polyurethane foams. J Therm Anal Cal. 2008;92:419–24.
18. Czerwosz E, Kowalska E, Wronka H, Radomska J: Patent notification nr P384 591. 2008.
19. Czerwosz E, Diduszko R, Dłużewski P, et al. Properties of Pd nanocrystals prepared by PVD method. Vacuum. 2008;82:372–6.
20. Gallagher PK, Gross ME. The thermal decomposition of palladium acetate, J Therm Anal. 1986;31:1231–41.
21. Fang PH. Diffusion mechanism of fullerene extraction from soot. Materials Research Innovations. 2000;4:1:60–3.
22. Hydrogen Sensor, Fast, Sensitive, Reliable and Inexpensive to Produce, 2006 Argonne National Laboratory, http://www.anl.gov/techtransfer/pdf/Profile_HydrogenSensor9_06.pdf.
23. Luongo K, Sine A, Bhansali S. Development of a highly sensitive porous Si based hydrogen sensor using Pd nano-structures. Sens Actuators B. 2005;111–112:125–9.